Available online at www.sciencedirect.com
SCIENCE DIRECT®
ELSEVIER
Journal of Nuclear Materials 329–333 (2004) 780–784
journal of nuclear materials
www.elsevier.com/locate/jnucmat

Effect of tungsten microstructure on blister formation by hydrogen and carbon mixed ion beam irradiation

T. Funabiki *, T. Shimada, Y. Ueda, M. Nishikawa

Department of Electronic, Information Systems, and Energy Engineering, Graduated School of Engineering, Osaka University, 2-1 Yamada-Oka, Suita, Osaka 565-0871, Japan

Abstract

Characteristics of blister formation for different types of tungsten (stress relieved W, recrystallized W, K-doped W, and La_2O_3-doped W) were studied by hydrogen and carbon mixed ion beam irradiation (1 keV H_3^+). In the carbon concentration in the ion beam of ~0.1%, no significant blisters were formed on the surface. However, many blisters of various sizes (from 1.0 μm to several hundred μm) were formed with carbon concentration of ~0.7%. These characteristics were observed for all samples. For the stress relieved W and K-doped W, blisters are round shapes, whose sizes ranged from 1 μm to several hundred μm in diameter. For the recrystallized W and La_2O_3-doped W, blisters are irregular shapes, whose sizes are almost the same from 20 to 50 μm in diameter. These similarities in blister shapes could be related to microstructure of the samples.

1. Introduction

In a development of fusion devices like ITER, selection of plasma facing materials is one of the key issues. In current plans for ITER, tungsten and carbon are candidate materials in the diverter [1,2]. In this case, carbon is eroded and diffuses into the edge plasma. It is expected that the tungsten will be irradiated with carbon impurity ions, as well as the deuterium and tritium fuel ions. Then a mixed layer of tungsten and carbon is formed on tungsten surface. Therefore, it is important to study the effect of this mixed layer on implanted hydrogen behavior in wall materials.

In order to investigate the effect of material mixing of carbon and tungsten, studies of ion irradiation effects on pure rolled tungsten were performed with hydrogen and carbon mixed ion beam [3–5]. As a result, it was found that blister characteristics of tungsten were dependent on carbon concentration in hydrogen beams and sample temperatures. As the carbon concentration was increased, blister characteristics such as sizes and the number were increased. For sample temperatures between 388 and 873 K, the size and number of blisters were a maximum at 653 K. However, the effects of microstructures and doped materials on blister formation in tungsten are not yet clear.

In this study, hydrogen and carbon mixed beam irradiation experiments with various tungsten samples such as pure tungsten materials (rolled and recrystallized) and K and La_2O_3-doped tungsten material have been conducted to clarify these effects.

2. Experiment

Experiments were performed with a high flux ion beam test device (HiFIT). This device employs on ECR discharge ion source to generate source plasmas. Plasma ions are extracted by three multiaperture spherical electrodes. Details of the HiFIT were described in Refs. [6–8].

In this study, hydrogen is used as the working gas. Ion beam components were mainly H_3^+ (70–80%). Beam energy, flux, and fluence were 1.0 keV, ~4.0×10^{20} H^+/m^2 s,

* Corresponding author. Tel.: +81-6 6877 5111x3675; fax: +81-6 6879 7867.
E-mail address: funaviki@st.eie.eng.osaka-u.ac.jp (T. Funabiki).

0022-3115/$ - see front matter
doi:10.1016/j.jnucmat.2004.04.174

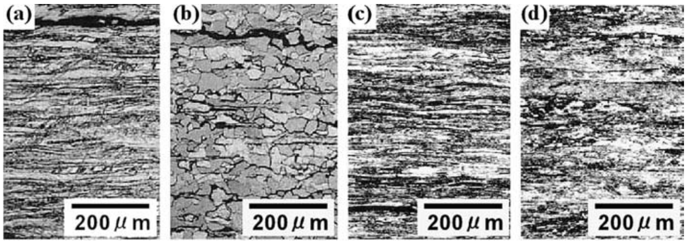

Fig. 1. Microstructure of four types of tungsten samples: (a) stress relieved W, (b) recrystallized W, (c) K-doped W, and (d) La_2O_3-doped W.

and $\sim 10^{25}$ H^+/m^2, respectively. In order to add carbon impurity to the hydrogen beam, graphite plates were put inside the ion source. Carbon impurities in the beam were extracted as hydrocarbon ions (CH_x^+, $C_2H_x^+$). The concentration of carbon ions can be controlled from 0.07% to 1.0% by changing the size of the graphite plates.

Four types of tungsten samples have been used. All samples were made by A.L.M.T.co, with a size of 10×20 mm and 1.0 mm thickness. Surfaces of the samples were mirror polished.

(i) Stress relieved W, with purity 99.99 wt%. Pure hot-rolled tungsten was annealed at 1173 K for 0.5 h in a hydrogen atmosphere. This sample had a laminar microstructure with thin grains parallel to the surface, as shown in Fig. 1(a).
(ii) Recrystallized W, with purity 99.99 wt%. Pure hot-rolled tungsten was annealed at 1573 K for 1.0 h in vacuum. Grains grew to average sizes of 20–30 μm. Microstructure was disordered, as shown in Fig. 1(b).
(iii) K-doped W (28 ppm K, 22 ppm Al), with the same heat treatments as stress relieved W. The microstructure characteristic was laminar, as shown in Fig. 1(c).
(iv) La_2O_3-doped W (0.96% La_2O_3), with the same heat treatments as stress relieved W. The microstructure was somewhat disordered, as shown in Fig. 1(d).

Samples were heated to temperatures between 653 and 823 K by an IR-Heater. The sample temperature was measured using a thermocouple inserted in a copper holder, which was attached to the back surface of the sample. Irradiated surfaces of samples were observed using a scanning electron microscopy (SEM).

3. Results and discussion

3.1. Dependence of blister formation on carbon concentration and sample temperature

Blister characteristic for the four materials were observed as a function of carbon concentration in the hydrogen ion beam and the sample temperature. In general, the dependence on carbon concentration and temperature is similar for all four materials. Therefore, results for stress relieved W are only shown. Fig. 2(a) and (b) shows SEM images of the irradiated regions of

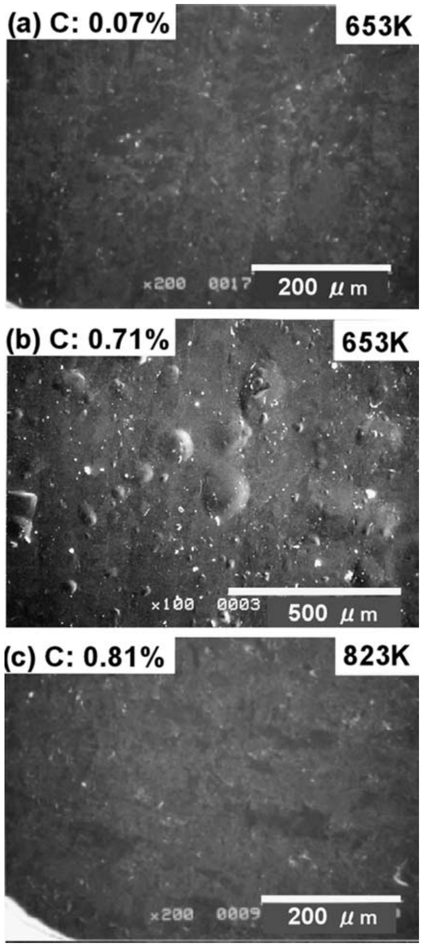

Fig. 2. SEM images of the stress relieved W after irradiation (a) at 653 K, and 0.07% C, (b) at 653 K, and 0.71% C, and (c) at 823 K, and 0.81% C. Irradiation beam energy and fluence were 1 keV H_3^+ and 1.0×10^{25} H/m^2.

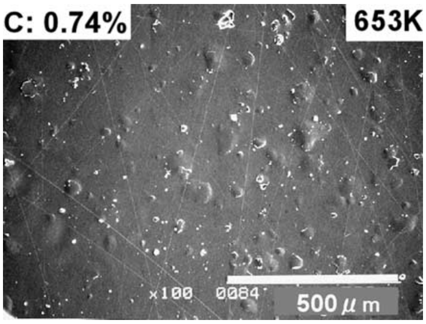

Fig. 3. SEM image of the recrystallized W after irradiation at 653 K, and 0.74 % C. Irradiation beam energy and fluence were 1 keV H_3^+ and 1.0×10^{25} H/m^2.

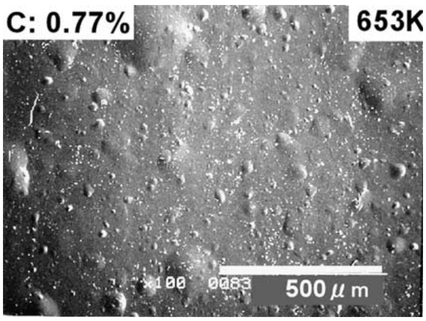

Fig. 4. SEM image of the K-doped W after irradiation at 653 K, and 0.77% C. Irradiation beam energy and fluence were 1 keV H_3^+ and 1.0×10^{25} H/m^2.

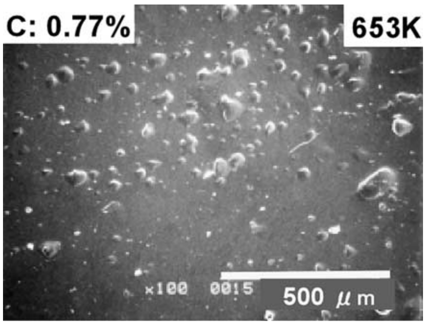

Fig. 5. SEM image of the La_2O_3-doped W after irradiation at 653 K, and 0.77% C. Irradiation beam energy and fluence were 1 keV H_3^+ and 1.0×10^{25} H/m^2.

stress relieved tungsten, after irradiation at 1.0 keV H_3^+, and 653 K. The beam fluence was about 1.0×10^{25} H$^+$/m^2. The carbon concentration in the mixed ion beam was 0.07% and 0.80%. When the carbon concentration was 0.07%, as shown in Fig. 2(a), no significant blisters were formed on the surface. However, many blisters of various sizes (from 1.0 μm to several hundred μm) were formed with the carbon concentration of 0.71%, as shown in Fig. 2(b). As the carbon concentration was increased, size and number of blisters was increased. Fig. 2(c) is SEM image of a sample surface irradiated at 823 K at carbon concentration of 0.7–0.8%. It was found that no significant blisters were formed at 823 K. These blister characteristics, as shown in Fig. 2(a)–(c), were similar to those described in Refs. [3–5].

3.2. Effect of tungsten microstructure on blister formation

In this section, details of blister for the four different tungsten materials are described. About the behavior of C impurity at the surface, details are described in Ref. [4]. Figs. 2–5 show SEM images of the irradiated regions of the four types of material, for the case of irradiation at 1.0 keV H$^+$, 653 K, 1.0×10^{25} H$^+$/m^2, and carbon concentration 0.8%. For the stress relieved W, shown in Fig. 2(b), blisters are almost round shapes. Sizes of blisters ranged from 1 μm to several hundred μm in diameter. The number density of blisters was about 445 blisters/mm^2. For the recrystallized W, shown in Fig. 3, blisters formed are irregular shapes. Sizes of blisters are similar (several tens μm in diameter). The number density of blisters is about 141 blisters/mm^2. For the K-doped W, shown in Fig. 4, blisters are almost round shape. Size of blisters ranged from 1 μm to several hundred μm, and the number density of blisters was about 2100 blisters/mm^2. This number density was the highest of all types of samples, because there were a lot

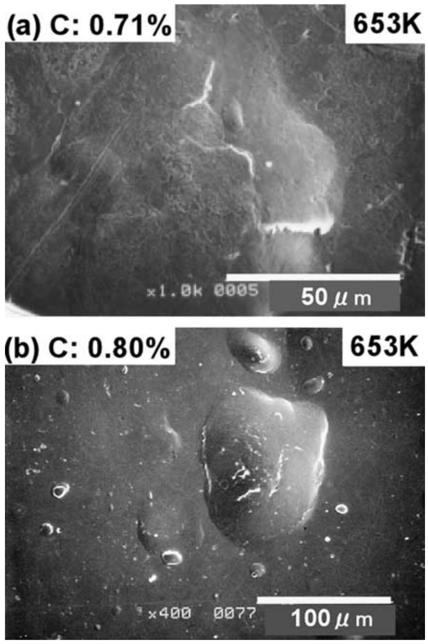

Fig. 6. SEM images of blisters formed on (a) stress relieved W, (b) K-doped W.

of blisters with sizes of 1–20 μm in diameter compared with other types of samples. For the La_2O_3-doped W, shown in Fig. 5, blisters formed are irregular shapes. Sizes of blisters are similar to those of recrystallized W. The number density of blisters was about 634 blisters/mm^2, and many cracks were found in the irradiated region on the sample surface.

In these results of SEM observation for four materials, several common characteristics of blisters for particular samples were found. For the stress relieved W and the K-doped W, blisters formed are round shapes and domed, as shown in Fig. 6. Large blisters with sizes of roughly 100 μm showed cracks on the surface. These similarities in blister shape could be related to microstructure. Both stress relieved W and K-doped W have laminar microstructure, shown in Fig. 1(a) and (c). The mechanism of blister formation may be as follows. The implanted hydrogen diffusing deeper into the material will eventually find trapping sites, which could be in grain boundaries [9]. Trapped hydrogen forms bubbles in the grain boundaries. In a laminar structure, two mechanisms of blister formation are possible. Firstly, the internal gas pressure of the trapped hydrogen increases, and causes plastic deformation on the sample surface to form round and domed shapes. Secondary, internal stress caused by retained hydrogen in grains is a driving force for blistering. We cannot conclude which mechanism is appropriate yet.

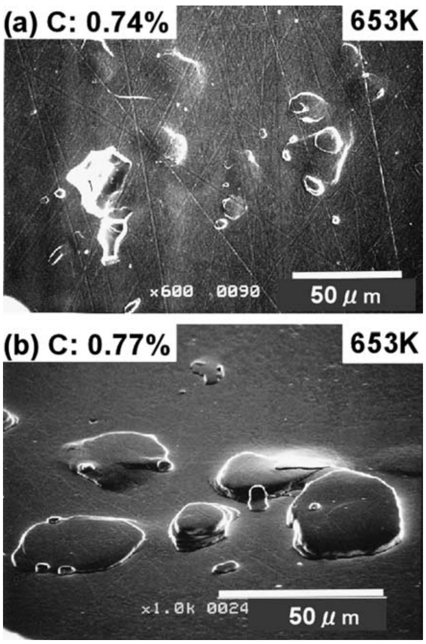

Fig. 7. SEM images of blisters formed on (a) recrystallized W, (b) La_2O_3-doped W.

For the recrystallized W and La_2O_3-doped W, blisters formed are irregular shapes (not dome shapes), as shown in Fig. 7(a) and (b). Almost all the blisters showed cracks at the edges. Sizes of blisters are similar (of order 20–50 μm in diameter). These similarities in blister shape could also be related to microstructure. Both recrystallized W and La_2O_3-doped W have disordered microstructures, shown in Fig. 1(b) and (d). The size of grains ranged from roughly 20 to 60 μm. This size of blisters corresponds to the size of grains in the microstructure. Therefore, in the case of re-crystallized W and La_2O_3-doped W, the mechanism of blister formation may be as follows. Bubbles are formed by trapped hydrogen in grain boundaries. As the number of bubbles increase, adhesion between grains gradually decreases. Internal stress may enhance this process. As a result, grains separate along grain boundaries.

4. Conclusions

In terms of blister formation, the dependence on carbon concentration in the hydrogen ion beam and the sample temperature is similar for all materials (stress relieved W, recrystallized W, K-doped W, and La_2O_3-doped W). When the carbon beam fraction was 0.07%, no significant blisters were formed on the surface. However, many blisters of various sizes (from 1.0 μm to several hundred μm) were formed for carbon concentration of 0.71%. At carbon concentration of 0.7–0.8%, blisters of various sizes were observed at 653 K, while no significant blisters were formed at 823 K. For the stress relieved W and K-doped W, blisters are round shapes, with a size rang from 1 μm to several hundred μm in diameter. For the recrystallized W and La_2O_3-doped W, blisters formed are irregular shapes. Sizes of blisters are similar (of order 20–50 μm in diameter). These similarities in blister shapes are related to the microstructure of the samples.

Acknowledgements

The authors are grateful to Professor Kurishita in Tohoku University for providing the samples.

References

[1] G. Federici, C.H. Skinner, J.N. Brooks, J.P. Coad, C. Grisolia, A.A. Haasz, A. Hassanein, V. Philipps, C.S. Pitcher, J. Roth, W.R. Wampler, D.G. Whyte, Nucl. Fusion 41 (2001) 1967.

[2] G. Janeschitz, A. Antipenkov, G. Federici, C. Ibbott, A. Kukushkin, P. Ladd, E. Martin, R. Tivery, Nucl. Fusion 42 (2002) 14.

[3] T. Shimada, H. Kikuchi, Y. Ueda, A. Sagara, M. Nishikawa, J. Nucl. Mater. 313–316 (2003) 204.
[4] T. Shimada, Y. Ueda, M. Nishikawa, Fusion Eng. Des. 66–68 (2003) 247.
[5] Y. Ueda, T. Shimada, M. Nishikawa, in: 19th IAEA Fusion Energy Conference, Lyon, France, 14–19 October 2002, IAEA-CN-94/FT/P1-15.
[6] T. Kawakami, T. Shimada, T. Yonezawa, Y. Ueda, M. Nishikawa, Rev. Sci. Instrum. 71 (2, part II) (2000) 1144.
[7] T. Shimada, T. Kawakami, Y. Ueda, A. Sagara, M. Nishikawa, J. Plasma Fusion Res. 3 (2000) 312.
[8] T. Shimada, Y. Ueda, A. Sagara, M. Nishikawa, Rev. Sci. Instrum. 73 (4) (2002) 1741.
[9] Rion A. Causey, J. Nucl. Mater. 300 (2002) 91.